

## Impact of Organic Carbon on the Stability and Toxicity of Fresh and Stored Silver Nanoparticles

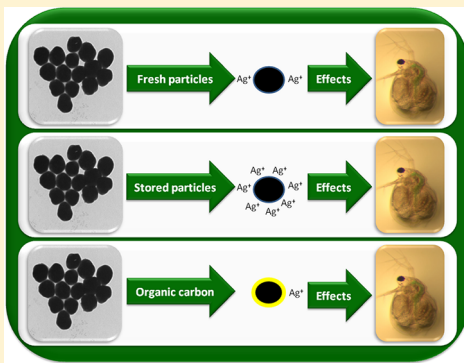
Alan J. Kennedy,<sup>\*,†</sup> Mark A. Chappell,<sup>†</sup> Anthony J. Bednar,<sup>†</sup> Adam C. Ryan,<sup>‡</sup> Jennifer G. Laird,<sup>†</sup> Jacob K. Stanley,<sup>†</sup> and Jeffery A. Steevens<sup>†</sup>

<sup>†</sup>U.S. Army Engineer Research and Development Center, Environmental Laboratory, 3909 Halls Ferry Road, Vicksburg, Mississippi, United States

<sup>‡</sup>HDR | HydroQual, Syracuse, New York, United States

### Supporting Information

**ABSTRACT:** Studies investigating the impact of particle size and capping agents on nanosilver toxicity in pristine laboratory conditions are becoming available. However, the relative importance of known environmental mitigating factors for dissolved silver remains poorly characterized for nanosilver in context with existing predictive toxicity models. This study investigated the implications of freshly prepared versus stored 20 and 100 nm nanosilver stocks to freshwater zooplankton (*Ceriodaphnia dubia*) in presence and absence of dissolved organic carbon (DOC). Results indicated that while the acute toxicity of nanosilver decreased significantly with larger size and higher DOC, storage resulted in significant increases in toxicity and ion release. The most dramatic decrease in toxicity due to DOC was observed for the 20 nm particle (2.5–6.7 fold decrease), with more modest toxicity reductions observed for the 100 nm particle (2.0–2.4 fold) and dissolved silver (2.7–3.1 fold). While a surface area dosimetry presented an improvement over mass when DOC was absent, the presence of DOC confounded its efficacy. The fraction of dissolved silver in the nanosilver suspensions was most predictive of acute toxicity regardless of system complexity. Biotic Ligand Model (BLM) predictions based on the dissolved fraction in nanosilver suspensions were comparable to observed toxicity.



### INTRODUCTION

Nanosilver (nanoAg) particles have many purported military, civil, and industrial applications, including medical devices, home appliances, water treatment, inks, and antimicrobial fabrics.<sup>1</sup> These applications are promising and should be fostered, though consideration to environmental fate and risks is needed. Many nanoAg applications are tailored to improve the health of mammals which are generally insensitive to silver; however, the free silver ion ( $\text{Ag}^+$ ) is highly toxic to freshwater fish and invertebrates through disruption of sodium–potassium transport that results in compromised ionoregulatory capacity and cardiac arrest.<sup>2–6</sup> While the availability of studies on the ecotoxicological effects of nanoAg is increasing in response to a proactive data call,<sup>7</sup> the full biological implications of nanoAg remain elusive. While most published studies report that dissolved Ag is more toxic than nanoAg suspensions,<sup>8–11</sup> a diversity of toxicity mechanisms for nanoAg is proposed<sup>8–14</sup> encompassing direct (reactive oxygen species production, membrane deformation, protein denaturation, DNA damage by free radicals) and indirect (particle oxidation and release of  $\text{Ag}^+$ ) effects.<sup>11,14</sup>

Inadequate particle characterization, large particle size distributions, unknown effects of coatings, and use of nonstandardized particle dispersion and testing methods in the expanding ecotoxicological database may present un-

certainty in environmental risk assessments. Further, the majority of studies have not investigated potential mitigating environmental factors in context with existing metal speciation and toxicity models, such as the Biotic Ligand Model (BLM).<sup>15</sup> The BLM characterizes the bioavailability and toxicity of metals (Cu, Ag, Zn, Cd) to aquatic organisms by calculating metal speciation and complexation with inorganic, organic and biotic ligands.<sup>16,17</sup> Important silver ligands the BLM considers include sulfides, chlorides and dissolved organic matter (DOC) in addition to cations ( $\text{Ca}^{2+}$ ,  $\text{Mg}^{2+}$ ,  $\text{Na}^+$ ) that can mediate toxicity by competition for binding sites. While it is known that environmental constituents mitigate dissolved Ag toxicity,<sup>2,4</sup> it is unclear if similar modifying effects on nanoAg toxicity will occur and thus the BLM cannot yet be calibrated to predict effects of nanoparticles. Recent studies have suggested that nanoAg toxicity decreases in the presence of sulfides<sup>18</sup> and natural organic matter.<sup>19</sup> Feeding rations, a form of organic matter, are reported to both reduce toxicity<sup>20</sup> or have no effect.<sup>21</sup> It is unclear from available work if the toxicity

**Received:** June 9, 2012

**Revised:** August 28, 2012

**Accepted:** September 5, 2012

reduction is related to complexation of the  $\text{Ag}^+$  ion in solution or a reduction in the toxicity of the particle itself.

In the current investigation, which supplements our previous study,<sup>8</sup> we investigated if the primary particle size, total available surface area, storage period of the nanoAg stock, and DOC controlled the acute toxicity of citrate-coated nanoAg suspensions. Dissolved organic carbon was selected as an interesting mitigating factor for two separate reasons; first, DOC reduces the agglomeration of nanoparticles such as carbon,<sup>22,23</sup>  $\text{CeO}_2$ <sup>24</sup> and  $\text{Ag}$ <sup>9,19,25–27</sup> through steric<sup>19</sup> or electrosteric<sup>22</sup> hindrance; second, DOC is known to reduce the toxicity of dissolved  $\text{Ag}$ .<sup>5</sup> We also considered the impact of concentration on particle aggregation to make inferences about the dispersion state of nanoAg at toxicologically relevant concentrations.

## MATERIALS AND METHODS

**Test Materials.** Citrate-capped nanoAg suspensions (1 g/L) with nominal sizes of 20 (NC20) and 100 (NC100) nm were obtained from a commercial source (NanoComposix, San Diego, CA). The toxicity of nanoAg was compared to dissolved Ag as reagent grade  $\text{AgNO}_3$  (CAS 7761–88–8, Sigma Aldrich, 204–390–50G, St. Louis, MO). Suwannee River reverse osmosis extracted natural organic matter (NOM, Cat No 1R101N, International Humic Substance Society, Atlanta, GA) was obtained as a powder to determine the influence of organic matter, quantified as DOC, on dissolved and nanoAg toxicity.

**Material Preparation.** Working nanoAg stocks (nominally 10 mg/L) were prepared in 100 mL ultrapure water (Milli-Q Plus ultrapure water system, 18.2 mΩ/cm, Billerica, MA) while bath sonicating for five minutes (Fisher Scientific model FS-60, 130W, Pittsburgh, PA). Aliquots of the working stocks were used in fate and bioassay experiments within one hour of preparation (hereafter referenced as fresh nanoAg). The remaining working stock was stored for 30 days (dark, 4 °C) in amber glass volumetric flasks to assess suspension characteristics and toxicity over time (hereafter referenced as stored nanoAg). The stored working stocks were bath sonicated for five minutes prior to use in bioassays. Natural organic matter (approximately 39% as DOC) was added to moderately hard reconstituted water (MHRW), formulated according to the U.S. Environmental Protection Agency (USEPA),<sup>28</sup> at the desired concentration (0, 4, 10 mg DOC/L). The specific conductance, ionic strength, chlorides and hardness concentrations of MHRW were 300  $\mu\text{S}/\text{cm}$ , 4.355 milli equivalents/L, 1.9 mg/L and 80 mg/L  $\text{CaCO}_3$ , respectively, which are important parameters for predicting the stability, complexation and speciation of nanoAg suspensions. The NOM solutions were magnetically stirred overnight and filtered at 0.45  $\mu\text{m}$  (HAWP047; Millipore, Bedford, MA) prior to use.

**Particle Characterization and Analytical Chemistry.** Nanosilver materials were characterized as described previously.<sup>8,29</sup> Briefly, primary particle size was determined by transmission electron microscopy (TEM, Zeiss 10CA, 60 kV, Oberkochen, Germany) through manual measurements of individual particles ( $\geq 200$ ) from 12 images using ImagePro Plus software (v7, Media Cybernetics Inc., Bethesda, MD). Particle characteristics were determined by dynamic light scattering (DLS; 635 nm laser; 90 Plus/BI-MAS, Brookhaven Instruments, Holtsville, NY) using an intensity-weighted autocorrelation function. Size was also determined using Field Flow Fractionation (PostNova F-1000 symmetrical flow FFF, Salt Lake City, UT) interfaced to an inductively coupled plasma

mass spectrometer (ICP-MS, Elan DRC-II, Perkin-Elmer, Waltham, MA). Functionally dissolved silver were determined by ultracentrifugation at 100 000g for 60 min (Beckman Optima XL-80K, Rotor 70.1 Ti, Brea, CA) and ICP-MS as previously described.<sup>8,29</sup> The term functionally dissolved is used since this method theoretically removes particles  $> 4$  nm; method efficacy was confirmed by deriving comparable dissolved fractions from integrations under void peaks of FFF-ICP-MS fractograms (which represent ions) relative to integrations of nanoAg particle peaks in the fractograms (see ref 8 and Supporting Information (SI), Table S3). In addition, the 10 mg/L working stocks were ultracentrifuged by this method and visually inspected for a pellet and clear supernatant. Aqueous samples (3% nitric acid v/v) were analyzed for Ag using ICP-MS and Graphite Furnace Atomic Absorption Spectroscopy following USEPA Methods 6020<sup>30</sup> and 7010,<sup>31</sup> respectively. Dissolved organic carbon was measured following USEPA Method 9060.<sup>32</sup>

**Fate Studies.** The aggregation kinetics of NC20 and NC100 were determined in MHRW at nominal concentrations of 0.9, 1.8, and 4.5 mg/L. These higher concentrations relative to bioassays (0–50  $\mu\text{g}/\text{L}$ ) were necessary to achieve adequate particle counts for DLS. Hydrodynamic diameter (HD) was determined at 0, 0.25, 0.5, 1, 2, 4, 24, and 48 h post interaction with MHRW. Modeling of the kinetic data was performed to determine how nanoAg concentration influenced aggregation after 48 h. In addition, 4.5 mg/L NC20 was similarly tested at 4 and 10 mg DOC/L to determine the impact of DOC on aggregation. Kinetic data were modeled by nonlinear least-squares fitting (Levenberg–Marquardt algorithm). While aggregation is typically modeled using a second order relationship, this requires knowledge of total particle concentration ( $N$  in units of  $\text{cm}^{-3}$ ). The hyperbolic function  $y = y_0 + a \times x/(b + x)$  was fit to the 48 h aggregation data (DLS) to model HD over a concentration range.

**Toxicity Bioassays.** Twenty-four acute (48 h) *Ceriodaphnia dubia* bioassays were conducted in accordance with USEPA<sup>28</sup> to compare the toxicity of NC20, NC100 and  $\text{AgNO}_3$ . The comparison consisted of four rounds of six simultaneously conducted bioassays. Each round involved three  $\text{AgNO}_3$  bioassays and three nanoAg bioassays conducted at each DOC concentration (0, 4, 10 mg/L). This was repeated for each nanoAg size for both freshly prepared stocks and stocks that were stored for 30-d. Moderately hard reconstituted water containing the desired DOC concentration was used as the diluent and control. After concentrations were prepared,  $\text{AgNO}_3$  and nanoAg were allowed 3 h to interact with DOC as in Naddy et al.<sup>33</sup> Mortality was assessed at 2, 24, and 48 h. Composite samples within each concentration were taken at 1 and 48 h for determination of total and dissolved silver.

**Data Analysis.** Response curves were plotted using SigmaPlot software (SPSS, Chicago, IL) on a log concentration scale. Fifty percent lethal concentration values (LC50s) and associated 95% confidence intervals (95% CIs) were determined by the trimmed Spearman-Karber method (ToxCalc 5.0, Tidepool Scientific Software, McKinleyville, CA) and statistical significance was defined as nonoverlapping CIs. Similarly, median lethal surface area (LSA50) values were determined by standardizing measured Ag concentration as total available surface area with each exposure level. Surface area ( $\text{mm}^2/\text{g}$ ) was calculated as the quotient of total volume (1 g silver,  $\rho = 10.49 \text{ g}/\text{cm}^3$ ) and individual particle volume (calculated from measured TEM diameters) to determine

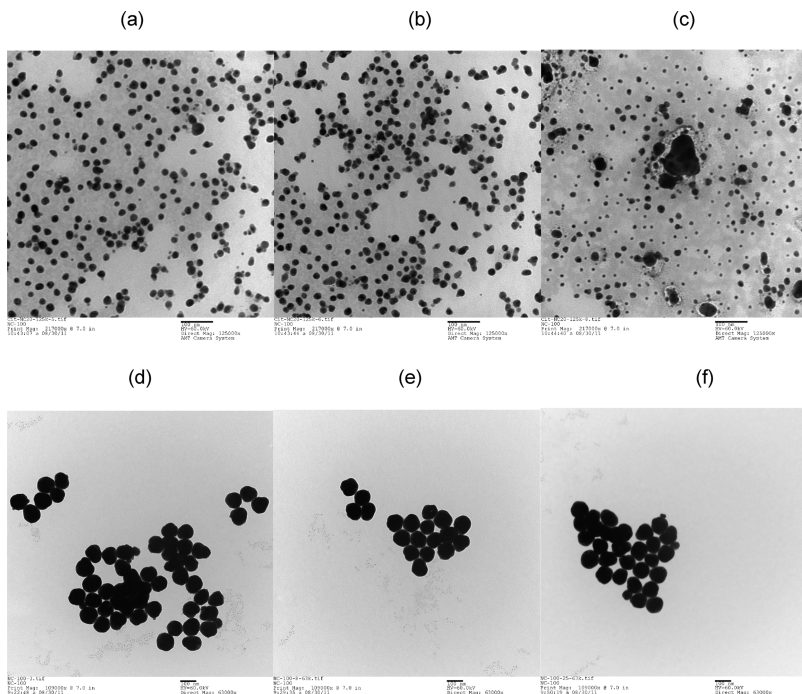


**Figure 1.** Transmission electron microscopy images of the 20 nm at 125 000 $\times$  (panels a–c) and 100 nm at 63 000 $\times$  (panels d–f) silver particle suspensions. The black scale bar for all is 100 nm.

particle number, which was multiplied by the calculated surface area of an individual particle. The percentage of silver concentration lost during the 48 h bioassays (measured as the reduction in total measurable Ag from the beginning to the end of testing) was calculated from the average of the highest three exposure concentrations. The BLM (using water quality parameters reported below) was applied in toxicity mode to provide predicted dissolved Ag LC<sub>50</sub> values for *C. dubia*.

## RESULTS AND DISCUSSION

**Particle Characterization.** The particles were circum-spherical (Figure 1), with mean measured primary particle sizes close to nominal (Table 1). The HDs (DLS, FFF) of the working stocks were larger than primary particle measurements,

as previously reported.<sup>8,25,29</sup> However, the DLS measurements for the 20 nm stock were larger than FFF measurements, likely skewed by the presence of rare but much larger (>100 nm) particles (Figure 1c). DLS is more influenced by larger particles than FFF since they scatter more light.<sup>34</sup> Measurement of Ag by ICP-MS following ultracentrifugation of freshly prepared stocks indicated that NC20 contained a higher relative concentration of dissolved Ag (or <4 nm, particles) compared to NC100 (Table 1). Storage of the NC20 and NC100 stocks resulted in an increase in dissolved Ag of 3.3 and 10.7-fold, respectively. The HDs of the NC20 and NC100 stocks by DLS slightly increased and broadened, respectively (Figure S1, SI), potentially due to an Ostwald ripening effect.

**Fate Studies.** The initial NC20 concentrations in MHRW were 585, 2218, and 4435  $\mu\text{g/L}$ . Aggregation increased rapidly over time while measurable Ag decreased (Figure 2). Hydrodynamic diameter (DLS) measurements indicated aggregate size and rates were greater with higher initial nanoAg concentration (Figure 2). After 48 h, size ranges were greater at the highest (172–1003 nm) relative to middle (100–572 nm), and lowest (45–268 nm) initial concentrations, which is intuitive since at lower concentrations particle-to-particle interaction frequency is lower.<sup>20</sup> Kinetic modeling of the 48 h HD indicated predicted sizes of 513, 457, and 246 nm for the high, middle and low concentrations systems, respectively. A significant fit ( $r = 0.999$ ,  $p = 0.013$ ) was obtained for these predicted aggregation sizes (Figure S2, SI), with the y-intercept (39 nm) being similar to the HD of the unaggregated stock (Table 1). This provides support for extrapolating to concentrations below 585  $\mu\text{g/L}$ . At a toxicologically significant concentration of 5  $\mu\text{g/L}$  (48 h LC<sub>50</sub> for NC20 described below), the hyperbolic model predicted a HD of 42 nm, suggesting little aggregation was expected after 48 h. Similar experiments conducted with NC100 resulted in relatively lower increases in aggregation (increase in HD from 90 to 160 nm). This supports previous conclusions that larger nanoparticles

**Table 1. Characterization of the Nanosilver Working Stocks after 0 and 30 Days of Storage<sup>a</sup>**

analysis	20 nm	100 nm
primary particle size (by TEM)	21 $\pm$ 4 (3–146)	102 $\pm$ 6 (51–137)
hydrodynamic diameter (by FFF)	25	104
hydrodynamic diameter (by DLS)	0 days storage 35 days storage	40 $\pm$ 5 (0.361 $\pm$ 0.001) 63 $\pm$ 2 (0.314 $\pm$ 0.003)
% dissolved silver in stock	0 days storage 35 days storage	5.3% 17.4%
		2.3% 24.6%

<sup>a</sup>Primary particle size was determined by transmission electron microscopy (TEM) and hydrodynamic diameter was determined by field flow fractionation (FFF) and dynamic light scattering (DLS). The baseline index and data retention for all DLS analyses exceeded 5.7 and 95%, respectively. Means and one standard deviation are provided. The polydispersity index of the dispersions is indicated in parentheses.

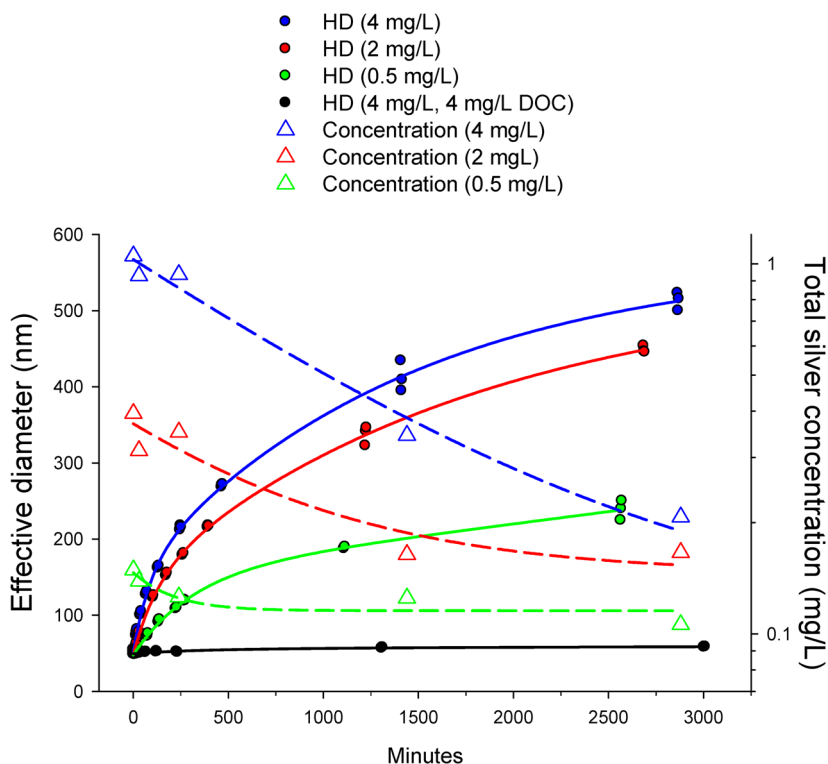


**Figure 2.** The hydrodynamic diameter (HD) and concentration of 20 nm nanosilver (NC20) at three different concentrations over approximately 3000 min. The impact of dissolved organic carbon (DOC) on HD is also shown. Filled circles and solid lines represent the HD data (left y-axis) while open triangles and dashed lines represent the concentration data (right y-axis). Concentration is plotted on a log10 scale.

aggregate less at high concentration due to lower mobility and less intense interaction frequency.<sup>34</sup> The presence of DOC appeared to stabilize particles even at high concentration, a finding supported by Gao et al.<sup>19</sup> NC20 (4435 µg/L) diameter increased only slightly in presence of 4 mg DOC/L (HD increased from 49 to 58 nm) and 10 mg DOC/L further inhibited aggregation (52 to 54 nm). Overall, results suggest aggregation is less important at lower, more toxicologically relevant concentrations over a 48 h bioassay exposure period compared to concentrations typically used in DLS analyses.

**Acute Toxicity.** Mean water quality parameters (ranges in parentheses) for bioassays were as follows; temperature:  $23.3 \pm 0.7$  (22.4–25.9) °C, conductivity:  $300 \pm 4$  (271–430) µS/cm, pH:  $8.09 \pm 0.11$  (7.30–8.85), dissolved oxygen  $8.0 \pm 0.9$  (6.1–8.8) mg/L. Most (90%) observed mortality occurred within the first 24 h of exposure to nanoAg and AgNO<sub>3</sub>, regardless of DOC. Nanosilver particle loss during the bioassays ranged from 4 to 51% (determined as the reduction in total measurable Ag from the beginning to the end of testing). The amount of loss depended on particle size, storage time and DOC (Figure S3, SI). Concentrations of the larger particle (NC100) were lost more rapidly than the smaller particle (NC20). An increase in storage time also led to a greater reduction in particle concentration. However, an increase in DOC concentration resulted in greater particle stability (less reduction in concentration) during the bioassays. Overall, these values are comparable to previously reported losses (6–52%) of a variety of nanoAg suspensions<sup>8</sup> but lower than other reporting (>90%;<sup>9</sup>).

**Relative Toxicity of Ionic Silver and Nanosilver.** The decrease in total Ag during the 48 h bioassays was relatively low for fresh NC20 ( $25 \pm 17\%$ ) but higher for NC100 ( $45 \pm 9\%$ ). Most ecotoxicology studies continue to report nanoAg toxicity

on a mass basis.<sup>8,9,11,14,21,35</sup> While it is understood that mass is unlikely to provide the best dose metric, we applied this convention to test the importance of dissolved Ag in determining acute toxicity and the impact of more complex media containing DOC; we later considered an alternative dosimetry. In absence of DOC (0 mg/L), the toxicity of dissolved Ag as AgNO<sub>3</sub> (mean 48 h LC<sub>50</sub> =  $0.7 \pm 0.5$  µg/L;  $n = 4$ ) was comparable to a range in *C. dubia* LC<sub>50</sub> values from the literature (0.3–0.9 µg/L;<sup>21,36</sup>) Dissolved Ag toxicity was significantly greater than both nanoAg suspensions as indicated by LC<sub>50</sub> values (Figure 3) and dose response curves (Figure S4a, SI). This finding is also supported in the literature.<sup>8–10</sup> Generally, our reported nanoAg LC<sub>50</sub> values (5–27 µg/L as total Ag) fall in the range of toxicity values for cladocerans (1–100 µg/L;<sup>8,9,14,20,21,37</sup>), although some report much lower (LC<sub>50</sub> > 500 µg/L;<sup>11</sup>) and higher (<1 µg/L;<sup>19,35</sup>) toxicity. Fresh NC20 (48 h LC<sub>50</sub> = 4.8 (4.5–5.1)) was significantly more toxic than the larger fresh NC100 (26.7 (26.2–27.3) µg/L) (Figure 3a). These LC<sub>50</sub> values are similar to those we previously reported for *Daphnia magna* exposed to the NC20 (5.3 (4.9–5.7) µg/L) and an 80 nm citrate nanoAg (17.7 (15.8–19.8)).<sup>8</sup> The smaller size of the 80 nm particle<sup>8</sup> relative to NC100 may explain its greater reported toxicity. Size dependent toxicity of nanoAg to aquatic organisms was previously reported in some<sup>8,38</sup> but not all<sup>14,19,35</sup> studies. By employing the ionic strength of MHRW, including chlorides, and considering the reactivity of eight potential silver species, the majority of silver in solution was calculated to be Ag<sup>+</sup> ( $\approx 80\%$ ), followed by AgCl<sub>(aq)</sub> ( $\approx 16\%$ ), AgSO<sub>4</sub><sup>-</sup> ( $\approx 0.6\%$ ). All other species (e.g., Ag(OH)<sub>2</sub><sup>-</sup>, AgCl<sub>2(aq)</sub>, AgCl<sub>3</sub><sup>2-</sup>, AgNO<sub>3(aq)</sub>, AgOH<sub>(aq)</sub>) were less than 0.5% of total silver (Figure S5, SI).

**Influence of DOC on Fresh Nanosilver Toxicity.** The present study applied additions of an isolated humic material to

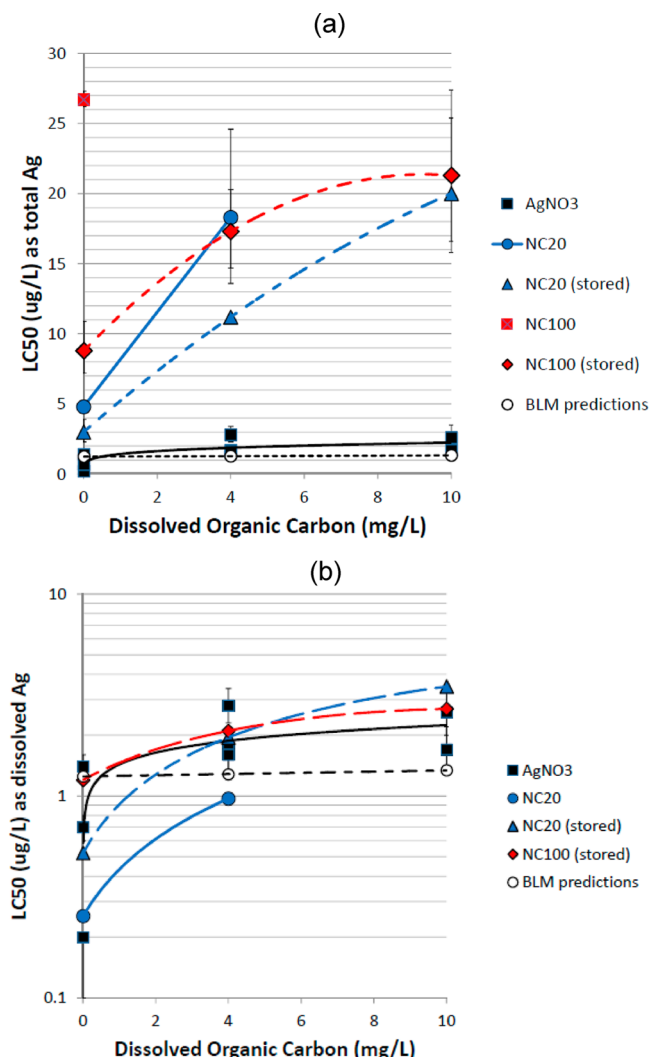


**Figure 3.** Lethal median concentrations (LC50) for *Ceriodaphnia dubia* exposed to nanosilver and ionic silver (as  $\text{AgNO}_3$ ) plotted against dissolved organic carbon. The 20 (NC20) and 100 (NC100) nm nanosilvers were tested both immediately (solid lines) and after approximately 30 days storage of the stock (dashed lines). Bars represent 95% percent confidence limits around the LC50 value. Panel (a) presents LC50 values based on total measurable silver while panel (b) presents LC50 values plotted on a log10 scale based on silver measured following ultracentrifugation. Both panels include biotic ligand model predictions.

create a controlled DOC gradient to test a dispersed, sol-based nanoAg in MHRW. Since water was filtered, measured DOC (4.1, 10.2 mg/L) concentrations were similar to TOC. A decrease in the toxicity of  $\text{AgNO}_3$  and both nanoAg sizes was observed as DOC increased (Figure 3). For dissolved Ag as  $\text{AgNO}_3$ , a significant toxicity reduction (2.7-fold decrease,  $p = 0.02$ ) was observed as DOC increased from 0 to 4 mg/L; this corresponded to a increase in mean LC50 values from  $0.7 \pm 0.5$  to  $1.9 \pm 0.6 \mu\text{g}/\text{L}$ . However, an increase in DOC from 4 to 10 mg/L did not result in a significant reduction in dissolved Ag toxicity ( $\text{LC50} = 2.2 \pm 0.6 \mu\text{g}/\text{L}$ ;  $p = 0.66$ ), as previously reported for fish.<sup>5</sup> For the fresh NC20 nanoAg, a relatively larger and significant, 3.8-fold toxicity reduction was observed as DOC increased from 0 to 4 mg/L (Figure 3a). While, insufficient mortality occurred to calculate LC50 values for NC20 at 10 mg DOC/L ( $\text{LC50} > 46.5 \mu\text{g}/\text{L}$ ; Figure S4c, SI)

and for NC100 at both 4 mg DOC/L ( $\text{LC50} > 41.4 \mu\text{g}/\text{L}$ ; Figure S4b, SI) and 10 mg DOC/L ( $>38.1 \mu\text{g}/\text{L}$ ; Figure S4c, SI), it was clear that the DOC significantly reduced the toxicity of these particles relative to water lacking DOC (Figure 3; Figure S4, SI). A toxicity reduction for a powder-based nanoAg material in DOC containing natural water was previously reported.<sup>19,35</sup> In the absence of DOC, this powder was heavily aggregated in suspension and had a very similar toxicity to dissolved Ag, which may suggest the presence of high ion concentrations. Powder-based nanoAg particles were previously reported to have greater dissolution potential and toxicity relative to sol-based nanoAg particles.<sup>37</sup>

The BLM provided estimates of the amount of dissolved Ag sorbed to DOC at the relative ionic strength of MHRW (SI, Figure S5c), which suggests clear potential for toxicity amelioration. It was previously reported that DOC coats nanoAg particles sufficiently to enhance stability,<sup>8,19,25–27</sup> though the mechanism for toxicity reduction is less straightforward relative to that of dissolved Ag. While complexation of released ions from the nanoAg particles can be assumed, it is not currently known whether DOC coatings on nanoAg particles passivate dissolution<sup>39</sup> or makes nanoAg less available for biouptake in the intestinal tract, as previously reported for cysteine-nanoAg complexes.<sup>40</sup>

**Influence of Storing Nanosilver on Toxicity.** In the absence of DOC, the toxicity of NC20 and NC100 increased significantly after the stocks were stored for 30 days (Figure 3a; Figure S4a, SI). The toxicity of NC20 and NC100 increased 1.6-fold ( $\text{LC50} = 3.0$  (2.3–3.9)  $\mu\text{g}/\text{L}$ ) and 3.0-fold ( $\text{LC50} = 8.8$  (7.2–10.9)  $\mu\text{g}/\text{L}$ ), respectively. This toxicity increase coincided with increased dissolved Ag in the stored stock (Table 1); further, similar increases in the fraction of dissolved Ag were observed in the stored NC20 working stock (17%) and bioassay treatments ( $17 \pm 6\%$ ) and in the NC100 working stock (24%) and bioassay treatments ( $22 \pm 14\%$ ). The increase in dissolved Ag during storage suggests continued dissolution in ultrapure water, likely due to lower concentration of stabilizing citrate. The associated increase in toxicity after storage suggests that dissolved Ag was the primary source of increased acute toxicity to *C. dubia*, as previously suggested for human stem cells.<sup>41</sup> Preliminary computational model results from interactions of citrate with nanoAg surfaces indicate that citrate chemically decomposes rapidly under slightly basic conditions (Dr. Frances Hill, Engineer Research and Development Center, personal communication). The presence of DOC may slow decomposition or recoat nanoAg by creating a dynamic equilibrium in which DOC replaces the citrate coating.<sup>42</sup>

**Influence of DOC on Stored Nanosilver Toxicity.** The toxicity of both stored NC20 and NC100 was significantly greater relative fresh nanoAg, allowing calculation of LC50 values (Figure 3a; SI Figure S4b,c) in all measured DOC concentrations (0, 4.6, 10.4 mg/L). The greatest toxicity reduction with increased DOC was observed for NC20 at 10 mg (6.7-fold) and 4 mg (3.7-fold) DOC/L, followed by  $\text{AgNO}_3$  (2.7 to 3.1-fold) and NC100 (1.7 to 2.4-fold). While a relatively small reduction in NC100 and  $\text{AgNO}_3$  toxicity was observed as DOC increased from 4 to 10 mg/L (Figure 3a), as previously observed for fresh nanoAg and reported for dissolved Ag,<sup>5</sup> the toxicity of stored NC20 continued to decrease as DOC increased from 4 to 10 mg/L (Figure 3a). The reason for this difference is unclear, since DOC both complexes disassociated ions<sup>5</sup> and coats nanoAg.<sup>19,25–27</sup> Potential explanations worthy of further research include inadequate DOC availability at 4

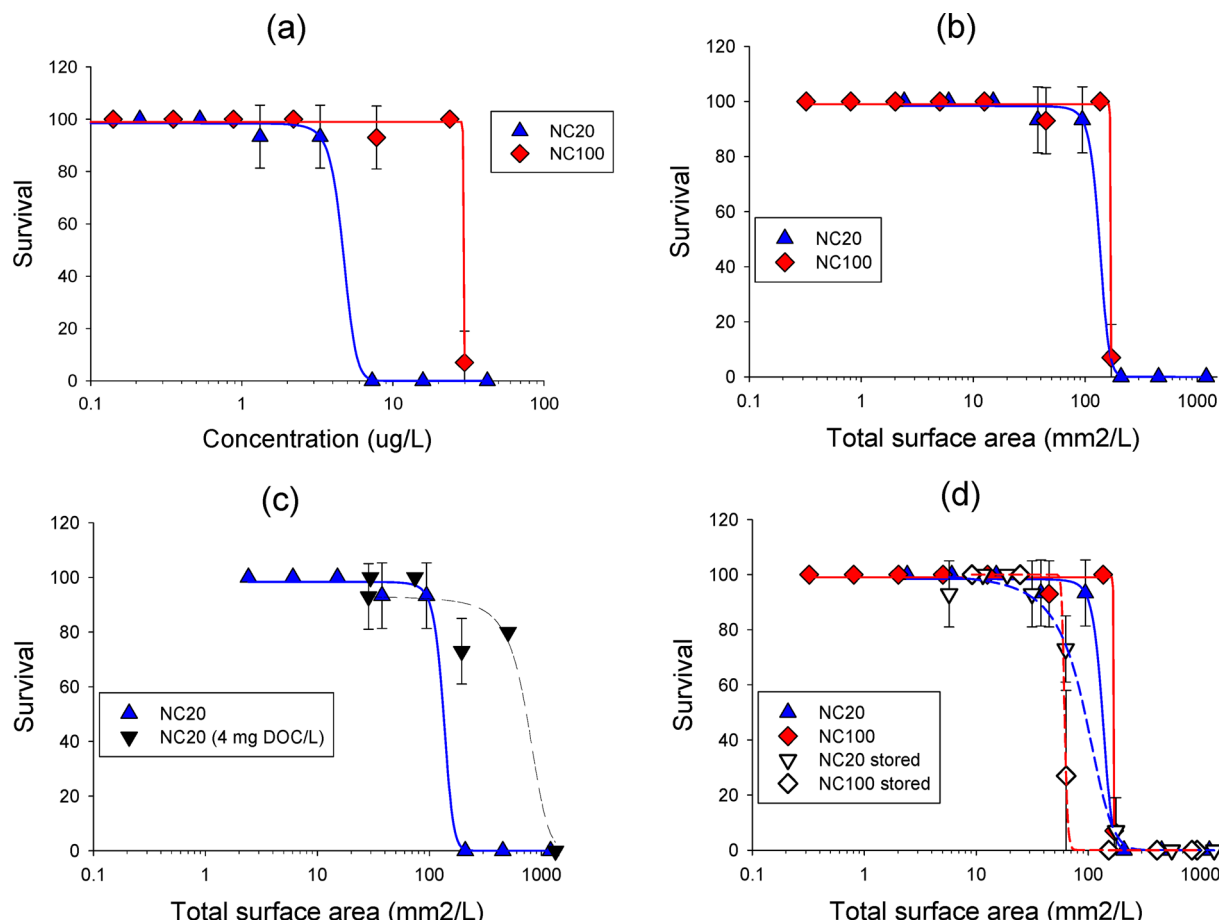


**Figure 4.** Dose response for 20 (NC20) and 100 (NC100) nm silver particles. Note that the *x*-axis uses a log10 scale. At 0 mg DOC/L, expression of survival response to dose by total mass (a) of fresh nanosilver is improved by standardization to total surface area (b). However, toxicity standardization by surface area was less successful when NC20 was in the presence of 4 mg DOC/L (c) or when materials were stored for approximately 30 days (d). Bars represent one standard deviation from the survival mean.

mg/L to fully coat the much greater total surface area of NC20 relative to NC100 (at equal mass concentration); insufficient complexation of ions due to the faster ion release kinetics from the smaller particle<sup>12,43</sup> and related rapid onset of Ag toxicity;<sup>8</sup> or more effective ion delivery of small particles at low ligand concentrations through attachment to the organism (while Ag<sup>+</sup> in solution is more efficiently complexed).<sup>39,44</sup> In addition, the capacity of 4 mg DOC/L to reduce stored NC20 toxicity may be further limited by the higher initial concentration of dissociated ions relative to fresh NC20 (Table 1). Differences in ion release kinetics are relevant since previous research supports a necessary interaction time between Ag<sup>+</sup> and DOC to realize full toxicity reduction.<sup>33</sup> Further, even as the stored 10 mg/L NC20 stock comes to equilibrium ( $K_{sp}$ ), additional dissolution is likely as the particle stock is diluted into MHRW and complexed by DOC (Figure S6, SI). Thus, while the 3 h equilibration before *C. dubia* addition was sufficient to maximize AgNO<sub>3</sub> and NC100 toxicity reduction at 4 mg DOC/L, additional DOC (10 mg/L) was required to reduce NC20 toxicity. In any case, the toxicities of NC20 and NC100 became more similar in the stored stocks as DOC increased from 0 to 10 mg/L (Figure 3 and SI Figure S4b), suggesting equilibration time may be more important than primary particle size.

**Relating Dose to Response.** As previously discussed, nanoAg toxicity (0 mg DOC/L) expressed on a total Ag

mass basis (Figure 4a) resulted in a 5.6-fold difference in LC50 values for NC20 and NC100, confirming the inadequacy of mass-based dosimetry.<sup>8</sup> Others<sup>38,45</sup> have suggested that surface area dosimetry has promising potential for standardizing nanoparticle toxicity; our results suggest total surface area provided an improved dosimetry for fresh nanoAg (0 mg DOC/L). The surface area normalized dose-response curves nearly overlaid (Figure 4b), eliciting only a 1.2-fold difference in LSA50 values (NC20 = 125 (106–147); NC100 = 153 (150–156) mm<sup>2</sup>/L). It remains unclear if this dose metric was more successful due to standardization to a direct particle effect or due to an indirect, covarying factor (greater ion release rate from a higher total surface area). Theoretically, based on thermodynamic solubility constants ( $K_{sp}$ ), the greater surface area of smaller particles may provide a faster release of ions and acquisition of system saturation of dissolved silver, which is supported in the literature.<sup>12,37</sup>

An issue with the surface area dose metric was that it appeared to be confounded with system complexity. For example, when *C. dubia* was exposed to fresh NC20 at 4 mg DOC/L, the LSA50 value increased 4.3-fold (531 (388–725) mm<sup>2</sup>/L) relative to the 0 mg DOC exposure (Figure 4c). Thus, DOC induced a fundamental change to the exposure, such as coating of the particles that prevented direct contact with the biotic ligand or reduced ion release and bioavailability.<sup>39</sup> Additionally, after nanoAg stocks were stored (Figure 4d), a

1.7-fold difference in LSA<sub>50</sub> values was determined (NC20 = 86 (66–112); NC100 = 50 (41–62) mm<sup>2</sup>/L). This is likely a result of the increased fraction of ions in the stored stocks, although it must be recognized that the increased HD of the stored NC20 may suggest lower than expected surface area (Table 1). Finally, storage of the initially less toxic (by mass) NC100 resulted in its toxicity becoming similar to NC20 based on LC<sub>50</sub> values (Figure 3a, Figure S4b, SI). This suggests that differences in handling, storage time and preparation of citrate coated nanoAg could mask size or surface area dependent effects if materials are not tested in the same state of equilibration.

Previous authors have presented seemingly conflicting conclusions that nanoAg toxicity was relatable to free ions in test media,<sup>8,10–14,37,44</sup> that the free ion failed to explain all toxicity<sup>8,9,46</sup> or that the mode of action was unique relative to that of the dissolved Ag based on genetic expression.<sup>47</sup> This may relate to differences in the nanoAg stocks (powder vs sol), type of coating, sonication procedures,<sup>48</sup> aggregation state and whether the exposure was anaerobic or aerobic.<sup>44</sup> Sotiriou and Pratsinis<sup>12</sup> suggested that the antimicrobial activity of small nanoAg particles was dominated by ion release but the particle itself became more important in determining antimicrobial activity for larger nanoAg sizes. It must also be recognized that the mechanism of nanoAg toxicity may vary between different model species. Yang et al.<sup>13</sup> observed that most studies concluding that the nanoparticle was most important for determining toxicity employed cell models while studies that related toxicity to dissolution tested multicellular organisms.

In more complex systems where organic matter is present or when dissolution is allowed to come into equilibrium, the initial differences in size or surface area dependent toxicity of the nanoparticles may become less important (Figure 3). For instance, while there was a 5.6-fold difference in fresh NC20 and NC100 toxicity at 0 mg DOC/L (Figure 3a; filled points), the toxicity of these two particles was only 2.9-fold different after 30 days storage and statistically indistinguishable when stored and tested in 10 mg DOC/L media (Figure 3a). DLS analysis of the stocks indicated the mean HD did not change substantially for aggregation state or surface area to explain this convergence in toxicity. However, when toxicity was expressed based on measurable Ag following ultracentrifugation (dissolved Ag), the resulting 48 h LC<sub>50</sub> values for both the fresh and stored NC20 and NC100 suspensions were similar to AgNO<sub>3</sub> toxicity (Figure 3b) and BLM toxicity predictions for dissolved Ag (Figure 3b). These data suggest the dissolved Ag, which may covary with the total surface area of the suspension, is important for predicting acute toxicity. Further, additional dissolution during the bioassay must be considered (refs 8,10 and SI Figure S6).

**Application of Biotic Ligand Model.** Others<sup>18</sup> reported that the BLM was predictive of dissolved Ag toxicity but not nanoAg toxicity. In the present study, the 48 h dissolved LC<sub>50</sub> values for *C. dubia* predicted by the BLM were remarkably consistent with the LC<sub>50</sub> values when expressed on the basis of dissolved Ag (Figure 3b), suggesting that the nanoAg toxicity is closely related to dissolved Ag.

In summary, the current investigation provided evidence that while citrate capped nanosilver particles aggregated rapidly at high concentrations (>1000 µg/L), aggregation and sedimentation at toxicologically relevant concentrations (<25 µg/L) was comparatively small. Bioassays clearly demonstrated an inverse relationship between nanoAg particle size and toxicity

that was relatable to both the total available surface area of particles in suspension and the dissolved fraction of Ag in solution, which are likely covarying factors. However, additional considerations that are critical for determining the toxicity nanoAg suspensions include ion release associated with long storage periods and environmentally relevant mitigating factors such as DOC, which was shown to increase the stability but decrease toxicity of nanoAg particles. Others<sup>18</sup> reported that the BLM was predictive of dissolved Ag toxicity but not nanoAg toxicity. In the present study, the 48 h dissolved LC<sub>50</sub> values for *C. dubia* predicted by the BLM were remarkably consistent with the LC<sub>50</sub> values when expressed on the basis of dissolved Ag (Figure 3b), suggesting that the nanoAg toxicity is closely related to dissolved Ag.

## ASSOCIATED CONTENT

### Supporting Information

Supporting information includes data on the fresh and stored stocks (Figure S1), a fit of aggregation versus starting concentration (Figure S2), total silver concentrations during bioassays (Figure S3), *C. dubia* dose response curves as a function of silver concentration and DOC (Figure S4), silver speciation calculations during bioassays (Figure S5) and dissolved concentrations during bioassays (Figure S6). This material is available free of charge via the Internet at <http://pubs.acs.org>.

## AUTHOR INFORMATION

### Corresponding Author

\*Phone: 601-634-3344; fax: 601-634-2263; e-mail: Alan.J.Kennedy@usace.army.mil.

### Notes

The authors declare no competing financial interest.

## ACKNOWLEDGMENTS

This research was funded by the U.S. Army Environmental Quality Research Program (Dr. Elizabeth Ferguson, technical director). Permission was granted by the Chief of Engineers to publish this information. We thank Drs. Chris Detzel and Dr. Matthew Hull (NanoSafe) and Ms. Ashley Harmon (ERDC) for TEM analysis. Drs. Frances Hill, David Johnson and three anonymous reviewers provided thoughtful comments.

## REFERENCES

- (1) Tolaymat, T. M.; El Badawy, A. M.; Genaidy, A.; Scheckel, K. G.; Luxton, T. P.; Suidan, M. An evidence-based perspective of manufactured silver nanoparticle in synthesis and applications: A systematic review and critical appraisal of peer-reviewed scientific papers. *Sci. Total Environ.* **2010**, *408*, 999–1006.
- (2) *Silver in the Environmental: Transport, Fate and Effects*; Andren, A. W., Bober, T. W., Eds.; Society of Environmental Toxicology and Chemistry: Pensacola, FL, 2002.
- (3) Ratte, H. T. Bioaccumulation and toxicity of silver compounds: A review. *Environ. Toxicol. Chem.* **1999**, *18*, 89–108.
- (4) Hogstrand, C.; Wood, C. M. Toward a better understanding of the bioavailability, physiology, and toxicity of silver in fish: Implications for water quality criteria. *Environ. Toxicol. Chem.* **1998**, *17*, 547–561.
- (5) Erickson, R. J.; Brooke, L. T.; Kahl, M. D.; Venter, F. V.; Harting, S. L.; Markee, T. P.; Spehar, R. L. Effects of laboratory test conditions on toxicity of silver to aquatic organisms. *Environ. Toxicol. Chem.* **1998**, *17*, 572–578.

- (6) Ferguson, E. A.; Hogstrand, C. Acute silver toxicity to seawater acclimated rainbow trout: Influence of salinity on toxicity and silver speciation. *Environ. Toxicol. Chem.* **1998**, *17*, 589–593.
- (7) Blaser, S. A.; Scheringer, M.; MacLeod, M.; Hungerbuhler, K. Estimation of cumulative aquatic exposure and risk due to silver: Contribution of nano-functionalized plastics and textiles. *Sci. Total Environ.* **2008**, *390*, 396–409.
- (8) Kennedy, A. J.; Hull, M. S.; Bednar, A. J.; Goss, J. D.; Gunter, J. C.; Bouldin, J. L.; Vikesland, P. J.; Steevens, J. A. Fractionating nanosilver: Importance for determining toxicity to aquatic test organisms. *Environ. Sci. Technol.* **2010**, *44*, 9571–9577.
- (9) Griffitt, R. J.; Luo, J.; Gao, J.; Bonzongo, J. C.; Barber, D. S. Effects of particle composition and species on toxicity of metallic nanomaterials in aquatic organisms. *Environ. Toxicol. Chem.* **2008**, *27*, 1972–1978.
- (10) Navarro, E.; Piccapietra, F.; Wagner, B.; Marconi, F.; Kaegi, R.; Odzak, N.; Sigg, L.; Behra, R. Toxicity of silver nanoparticles to *Chlamydomonas reinhardtii*. *Environ. Sci. Technol.* **2008**, *42*, 8959–8964.
- (11) Zhao, C. M.; Wang, W. X. Comparison of acute and chronic toxicity of silver nanoparticles and silver nitrate to *Daphnia magna*. *Environ. Toxicol. Chem.* **2011**, *30*, 885–892.
- (12) Sotiriou, G. A.; Pratsinis, S. E. Antibacterial activity of nanosilver ions and particles. *Environ. Sci. Technol.* **2010**, *44*, 5649–5654.
- (13) Yang, X.; Gondikas, A. P.; Marinakos, S. M.; Auffman, M.; Liu, J.; Hsu-Kim, H.; Meyer, J. Mechanism of silver nanoparticle toxicity is dependent on dissolved silver and surface coating in *Caenorhabditis elegans*. *Environ. Sci. Technol.* **2012**, *46*, 1119–1127.
- (14) Li, T.; Albee, B.; Alemayehu, M.; Diaz, R.; Ingham, L.; Kamal, S.; Rodrigues, M.; Bishnoi, S. W. Comparative toxicity study of Ag, Au, Ag-Au bimetallic nanoparticles on *Daphnia magna*. *Anal. Bioanal. Chem.* **2010**, *398*, 689–700.
- (15) Paquin, P. R.; Gorsuch, J. W.; Apte, S.; Batley, G. E.; Bowles, K. C.; Campbell, P. G. C.; Delos, C. G.; Di Toro, D. M.; Dwyer, R. L.; Galvez, F.; Gensemer, R. W.; Goss, G. G.; Hogstrand, C.; Janssen, C. R.; McGeer, J. C.; Naddy, R. B.; Playle, R. C.; Santore, R. C.; Schneider, U.; Stubblefield, W. A.; Wood, C. M.; Wu, K. B. 2002. The biotic ligand model: A historical overview. *Comp. Biochem. Physiol., Part C: Toxicol. Pharmacol.* **2002**, *133*, 3–35.
- (16) Di Toro, D. M.; Allen, H. E.; Bergman, H. L.; Meyer, J. S.; Paquin, P. R.; Santore, R. C. A biotic ligand model of the acute toxicity of metals I. Technical basis. *Environ. Toxicol. Chem.* **2001**, *20*, 2383–2396.
- (17) Tipping, E. 1994. WHAM—A chemical equilibrium model and computer code for waters, sediments, and soils incorporating a discrete site/electrostatic model of ion-binding by humic substances. *Comput. Geosci.* **1994**, *20*, 973–1023.
- (18) Choi, O.; Clevenger, T. E.; Deng, B.; Surampalli, R. Y.; Ross, L.; Hu, Z. 2011. Role of sulfide and ligand strength in controlling nanosilver toxicity. *Water Res.* **2011**, *43*, 1879–1886.
- (19) Gao, J.; Youn, S.; Hovsepian, A.; Llaneza, V. L.; Wang, Y.; Bitton, G.; Bonzongo, J. C. 2009. Dispersion and toxicity of selected manufactured nanomaterials in natural river water samples: Effects of water chemical composition. *Environ. Sci. Technol.* **2009**, *43*, 3322–3328.
- (20) Allen, H. J.; Impellitteri, C. A.; Macke, D. A.; Heckman, J. L.; Poynton, H. C.; Lazorchak, J. M.; Govindasamy, S.; Roose, D. L.; Nadagouda, M. N. Effects from filtration, capping agents, and presence/absence of food on the toxicity of silver nanoparticles to *Daphnia magna*. *Environ. Toxicol. Chem.* **2010**, *29*, 2742–2750.
- (21) Bielmyer, G. K.; Bell, R. A.; Klaine, S. J. Effects of ligand-bound silver on *Ceriodaphnia dubia*. *Environ. Toxicol. Chem.* **2002**, *21*, 2204–2208.
- (22) Kennedy, A. J.; Gunter, J. C.; Chappell, M. A.; Goss, J. G.; Hull, M. S.; Kirgan, R. A.; Steevens, J. A. Influence of nanotube preparation in aquatic bioassays. *Environ. Toxicol. Chem.* **2009**, *28*, 1930–1938.
- (23) Chappell, M. A.; George, A. J.; Dontsova, K. M.; Porter, B. E.; Price, C. L.; Zhou, P.; Morikawa, E.; Kennedy, A. J.; Steevens, J. A. Surfactive stabilization of multi-walled carbon nanotube dispersions with dissolved humic substances. *Environ. Pollut.* **2009**, *157*, 1081–1087.
- (24) Quik, J. T. K.; Lynch, I.; Van Hoecke, K.; Miermans, C. J. H.; De Schampelaere, K. A. C.; Janssen, C. R.; Dawson, K. A.; Stuart, M. A. C.; Van de Meent, D. Effect of natural organic matter on cerium dioxide nanoparticles settling in model fresh water. *Chemosphere* **2010**, *81*, 711–715.
- (25) MacCuspie, R. I.; Roger, K.; Patra, M.; Suo, Z.; Allen, A. J.; Martin, M. N.; Hackley, V. A. Challenges for the physical characterization of silver nanoparticles under pristine and environmentally relevant conditions. *J. Environ. Monit.* **2011**, *13*, 1212–1226.
- (26) Cumberland, S. A.; Lead, J. R. Particle size distributions of silver nanoparticles at environmentally relevant conditions. *J. Chromatogr., A* **2009**, *1216*, 9099–9105.
- (27) Fabrega, J.; Fawcett, S. R.; Renshaw, J. C.; Lead, J. R. Silver nanoparticle impact on bacterial growth: Effect of pH, concentration, and organic matter. *Environ. Sci. Technol.* **2009**, *43*, 7285–7290.
- (28) *Methods for Measuring the Acute Toxicity of Effluents and Receiving Waters to Freshwater and Marine Organisms*, EPA/ 812/R/02/012; U.S. Environmental Protection Agency, Office of Water: Washington, DC, 2002.
- (29) Poda, A. R.; Bednar, A. J.; Kennedy, A. J.; Harmon, A.; Hull, M.; Mitrano, D. M.; Ranville, J. F.; Steevens, J. Characterization of silver nanoparticles using flow-field flow fractionation interfaces to inductively coupled plasma mass spectroscopy. *J. Chromatogr., A* **2011**, *1218*, 4219–4225.
- (30) U.S. Environmental Protection Agency. *Methods for Evaluating Solid Waste, SW-846, Inductively Coupled Plasma Mass Spectrometry*, 6020A, February 2007.
- (31) U.S. Environmental Protection Agency. *Methods for Evaluating Solid Waste, SW-846, Graphite Furnace Atomic Absorption Spectroscopy*, 7010, February 2007.
- (32) U.S. Environmental Protection Agency. *Methods for Evaluation of Solid Waste, SW-846, Method 9060A, Total Organic Carbon*, November 2004.
- (33) Naddy, R. B.; Gorsuch, J. W.; Rehner, A. B.; McNerney, G. R.; Bell, R. A.; Kramer, J. R. Chronic toxicity of silver nitrate to *Ceriodaphnia dubia* and *Daphnia magna*, and potential mitigating factors. *Aquat. Toxicol.* **2007**, *84*, 1–10.
- (34) Romer, I.; White, T. A.; Baalousha, M.; Chipman, K.; Viant, M. R.; Lead, J. R. Aggregation and dispersion of silver nanoparticles in exposure media for aquatic toxicity tests. *J. Chrom A* **2011**, *1218*, 4226–4233.
- (35) McLaughlin, J.; Bonzongo, J. C. J. Effects of natural water chemistry on nanosilver behavior and toxicity to *Ceriodaphnia dubia* and *Pseudokirchneriella subcapitata*. *Environ. Toxicol. Chem.* **2012**, *31*, 168–175.
- (36) Rodgers, J. H.; Deaver, E.; Suedel, B. C.; Rogers, P. L. Comparative aqueous toxicity of silver compounds: Laboratory studies with freshwater species. *Bull. Environ. Contam. Toxicol.* **1997**, *58*, 851–858.
- (37) Lee, Y. J.; Kim, J.; Oh, J.; Bae, S.; Lee, S.; Hong, I. S.; Kim, S. H. Ion-release kinetics and ecotoxicology of silver nanoparticles. *Environ. Toxicol. Chem.* **2012**, *31*, 155–159.
- (38) Cowart, D. A.; Guida, S. M.; Shah, S. I.; Marsh, A. G. Effects of Ag nanoparticles on survival and oxygen consumption of zebra fish embryos, *Danio rerio*. *J. Environ. Sci. Health, Part A: Toxic/Hazard. Subst. Environ. Eng.* **2011**, *46*, 1122–1128.
- (39) Marambio-Jones, C.; Hoek, E. M. V. A review of the antibacterial effects of silver nanomaterials and potential implications for human health and the environment. *J. Nanopart. Res.* **2010**, *12*, 1531–1551.
- (40) Zhao, C. M.; Wang, W. X. Biokinetic uptake and efflux of silver nanoparticles in *Daphnia magna*. *Environ. Sci. Technol.* **2010**, *44*, 7699–7704.
- (41) Kittler, S.; Greulich, C.; Diendorf, J.; Koller, M.; Epple, M. Toxicity of silver nanoparticles increases during storage because of slow dissolution under release of silver ions. *Chem. Mater.* **2010**, *22*, 4548–4554.

- (42) Poda A. R.; Kennedy A. J.; Bednar, A. J. The effect of photoysis on the stability and toxicity of silver nanoparticles. In *Nanotechnology 2012: Bio Sensors, Instruments, Medical, Environment and Energy*; Nano Science and Technology Institute: Austin, TX, 2012; Vol. 3, pp 319–322, ISBN: 978-1-4665-6276-9
- (43) Zhang, W.; Yao, Y.; Siullivan, N; Chen, Y. Modeling the primary size effects of citrate-coated silver nanoparticles on their ion release kinetics. *Environ. Sci. Technol.* **2011**, *45*, 4422–4428.
- (44) Xiu, Z. M.; Ma, M.; Alvarez, J. J. Differential effect of common ligands and molecular oxygen on antimicrobial activity of silver nanoparticles versus silver ions. *Environ. Sci. Technol.* **2011**, *45*, 9003–9008.
- (45) Oberdorster, G.; Oberdorster, E.; Oberdorster, J. Nanotoxicology: An emerging discipline evolving from studies of ultrafine particles. *Environ. Health Perspect.* **2005**, *113*, 823–839.
- (46) Laben, G.; Nies, L. F.; Turco, R. F.; Bickham, J. W.; Sepulveda, M. S. The effects of silver nanoparticles on fathead minnow (*Pimephales promelas*) embryos. *Ecotoxicol.* **2010**, *19*, 185–195.
- (47) Griffitt, R. J.; Hyndman, K.; Denslow, N. D.; Barber, D. S. Comparison of molecular and histological changes in zebrafish gills exposed to metallic nanoparticles. *Toxicol. Sci.* **2009**, *107*, 404–415.
- (48) Taurozzi, J. S.; Hackley, V. A.; Wiesner, M. R. Ultrasonic dispersion of nanoparticles for environmental, health and safety assessment—Issues and recommendations. *Nanotoxicology* **2010**, *5*, 711–729.